

Application of a static surrogate model for the seismic analysis of multiple interconnected deep shafts, a case study

Carlos Menéndez-Vicente¹, José Concha-Riedel^{1,2}, Jörg Meier¹, Laurent Pitteloud¹

¹Gruner AG, Basel, Switzerland, carlos.menendez@gruner.ch; ²Universidad Adolfo Ibáñez, Viña del Mar, Chile

ABSTRACT: The computational requirements for detailed modelling of large and complex geotechnical structures under seismic loading make a full dynamic analysis prohibitive. In tunnel seismic design, static surrogate models based on the deformation method are often considered to overcome high computational costs and estimate internal forces and deformations of the structure. This paper explores the application of the deformation method to a case study of multiple interconnected deep shafts embedded in soft saturated soils located in a seismic prone area. A geometrically simplified version of the structure was modelled, and a fully dynamic simulation was performed under multidirectional seismic loading. By investigating the structural response, in particular the main 3D deformation modes and internal forces (i.e. bending, shear, axial), a set of prescribed displacements was calibrated to be used as boundary conditions at the edges of a surrogate model under static loading. This set of prescribed displacements was then applied to the geometrically complex full design model. This case study describes the procedure and highlights the challenges encountered in the analysis of deep shaft structures in the framework of a large-scale hydropower project. It presents the application of an existing method to a different field. The aim of this study is to assess the applicability of this approach as a preliminary seismic design strategy and to derive meaningful results for further investigation.

KEYWORDS: Finite elements, seismic loading, static surrogate, shaft, underground structures.

1 INTRODUCTION

The incorporation of computers into the calculation and modelling of structures in the last decades has greatly improved their analysis, allowing engineers to develop complex numerical simulations. However, even though computational capabilities have increased exponentially in the last years, the time required for running complex numerical models – or even dynamic simulations – can last over several weeks and even months, which may render this approach unfeasible.

Underground structures, mainly tunnels, subjected to seismic action are often analysed with the Seismic Deformation Method (SDM). This method seeks to measure the deformations on a soil mass induced by the seismic action, and to replicate them with a set of prescribed displacements applied to the model boundaries (Hashash et al., 2001; Wang & Munfakh, 2001; St. John & Zahrah, 1987). Underground structures are principally subjected to the imposed soil deformations triggered by the seismic loads. This approach differs from the pseudo-static analysis used for structures over the surface, which are exposed to the inertial forces caused by the seismic loads at ground level. Gaspari et al. (2011) applied the aforementioned method via a set of prescribed displacements to analyse the seismic tunnel response in the Istanbul metro line. Pescara et al. (2011) followed their research with analyses of the tunnel body under different seismic conditions. They evaluated the soil's shear deformations under a free field condition, which was used to estimate the ovalisation of the lining for dimensioning purposes.

The calculation of large and complex, even dynamic, Finite Element Models (FEM) requires significant time and computational resources. As such, the ability to perform e.g. additional sensitivity analyses to evaluate different model parameters, might become unfeasible. The use of simplified, smaller versions of the initial model, known as surrogate model, has become a popular technique among engineers to perform several low-cost simulations, which can later be used as inputs for complex models (Liu et al., 2024; Zheng et al., 2023; Asher et al., 2015). These models can be built via simulation and interpolation of parameters (probabilistic analysis and optimisation algorithms, e.g. Liu et al., 2024; Meier et al., 2009; Zheng et al., 2023) or by simplifying the structure and model conditions (Robinson et al., 2008). One of the simplifications might be as straightforward as to reduce the number of elements

in the mesh, or the amount of system variables (e.g. a reduction of the amount of material types).

This paper presents the seismic analysis of a highly complex structure based on multiple interconnected shafts embedded in soft saturated soils. Therefore, a surrogate simplified model of a single deep shaft excavation is implemented, for which a time history analysis of a design earthquake is conducted. The seismic-induced deformation results are then calibrated to a series of prescribed displacements on the boundaries of the model via the SDM. This set of prescribed displacements containing the worst-case shear (seismic) response was then used for a pseudo-static analysis of the complex FEM.

Driven by the computational limitations in numerical modelling, this study proposes the application of an existing method, originally developed for tunnel engineering, to a new field: the study of embedded shafts in soft saturated soils. It applies the SDM for seismic analysis and it presents modelling techniques to overcome complex geometries via surrogate modelling. The proposed methodology serves as an initial design strategy for complex structures exposed to seismic loads.

2 CASE STUDY

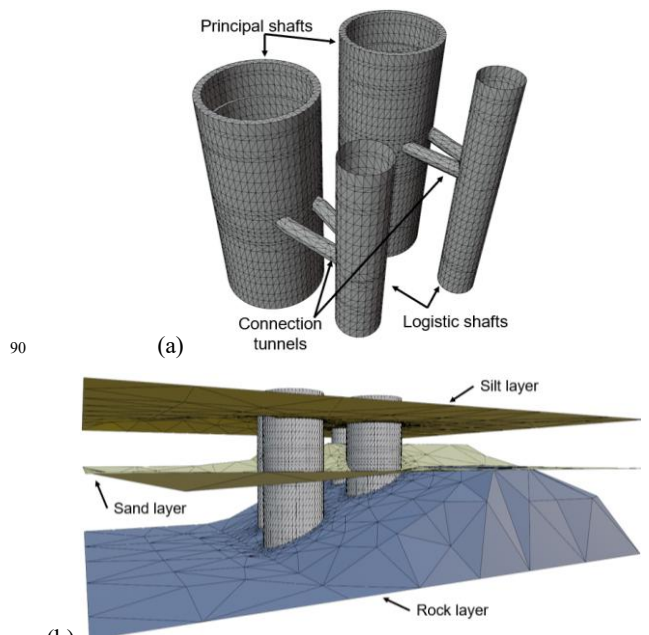
2.1 Structure

This paper is based on a case study of a hydropower infrastructure consisting of two principal shafts (49 m in diameter and 59 m of excavation depth) and two logistic shafts (19.5 m in diameter and 56 m in excavation depth). All shafts are built using 1.5 m thick rectangular sections of diaphragm walls (D-wall) with different embedment depths, depending on their distance to the bed rock. Below the foundation slab of both principal shafts, a series of 1.5 m diameter piles is added for additional support and foundation of the future structure. The principal shafts are connected to the logistic shafts via two small-diameter tunnels (7 m) each. These small-diameter tunnels are planned to be built using the soil freezing technique, once the four shafts are finalized. Figure 1a shows the 3D model of the structure and their principal components.

2.2 Hydrogeology

The soil consists of four major layers: a plastic silty clay, a medium dense silt, a dense sand, and a volcanic weathered rock. The three soil layers comprise the first 55 m of the site, while the rock can be found between 55 to 118 m below the surface

85 level, as it lays in an inclined plane (Figure 1b). The plastic silty
 86 clay and silt have considerable weak mechanical parameters
 87 (Table 1). The water table is located 7 m below the ground
 88 level, as this infrastructure seeks to pump seawater from a lake
 89 to an uphill reservoir.



91 (b)
 92 Figure 1. 3D model of the hydropower infrastructure: (a) structures of
 93 interconnected shafts and (b) soil layers.

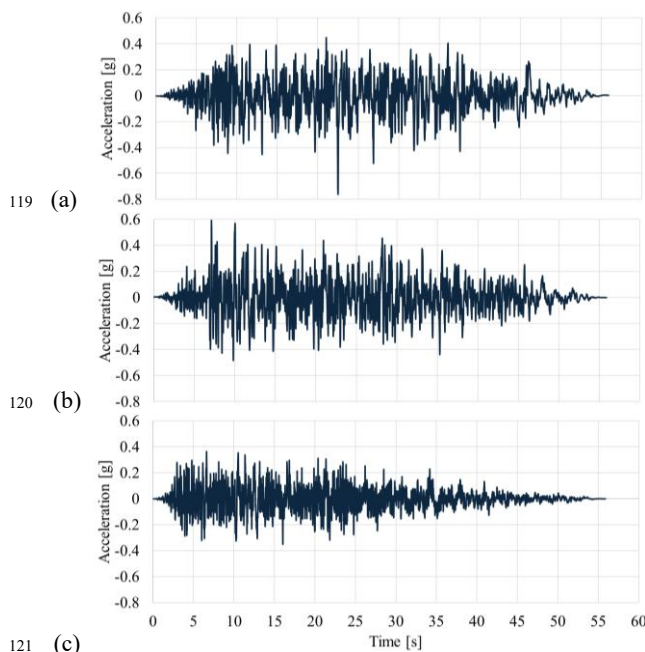
94 Table 1. Soil parameters (estimated).

Soil	γ_{sat} kN/m ³	E_{oed}^{ref} kN/m ²	E_{ur}^{ref} kN/m ²	c'_{ref} kN/m ²	ϕ' °
Plastic clay	20	5E2	2E3	5	15
Silt	20	2E3	5E3	10	18
Sand	21	15E3	45E3	5	26
Rock	23	300E3	900E3	50	25

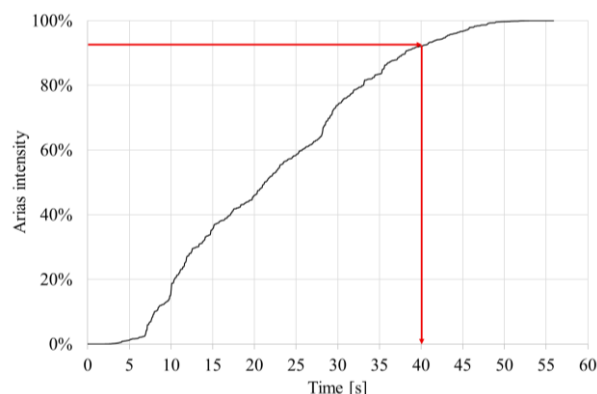
95 2.3 Seismic loads

96 The hydropower facility is planned to be constructed in a
 97 seismic active region of Southeast Asia. The dynamic analysis
 98 was performed for the following seismic input motions and
 99 corresponding return periods: Construction Earthquake (CE, 50
 100 years), Operating Basis Earthquake (OBE, 145 years), and
 101 Design Basis Earthquake (DBE, 475 years). For the CE
 102 analysis, the structure consists of the D-walls forming the shaft
 103 and stiffened with ring beams, the foundation piles, and a fully
 104 excavated pit without the foundation slab. This construction
 105 stage is the worst-case situation during construction with the
 106 weakest structure. In the final construction stage, the structure
 107 is stiffer due to the foundation slab, but it is subject to higher
 108 seismic loads (OBE and DBE). These different seismic events
 109 are intended to cover different hazard levels during construction
 110 (CE), and for the final stage (OBE, DBE), addressing the
 111 serviceability and ultimate conditions respectively. The present
 112 paper focuses on the representative results of the DBE analysis.

113 The seismic input motion for the time history analysis is a
 114 spectrally matched accelerogram of the Landers earthquake
 115 (Figure 2). To reduce computational costs, only the first 40
 116 seconds of the time history input were applied, reaching 95 %
 117 of the Arias intensity (Figure 3). This ratio is generally
 118 considered a conservative yet sufficient assumption.



121 (c)
 122 Figure 2. Acceleration time history (a, b) in both horizontal directions
 123 and (c) in vertical direction of the DBE seismic input.



124
 125 Figure 3. Analysis of the Arias intensity (the red line marks the 40
 126 seconds under consideration and the corresponding Arias intensity).

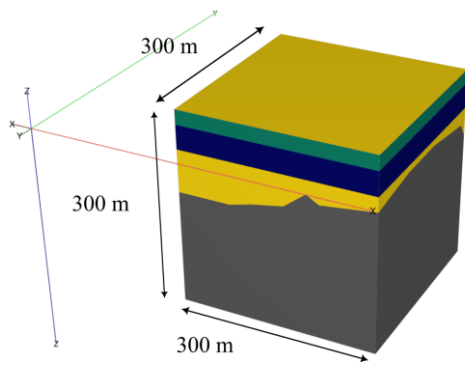
127 3 METHODOLOGY

128 3.1 General approach

129 The first approach to this case study was the development of a
 130 full design model with Plaxis 3D. This model covers all
 131 construction phases under static conditions. However, the dynamic
 132 calculation of this 3D FEM model with its complex
 133 geometry, soft saturated soil conditions (Table 1), and seismic
 134 multidirectional input motion (Figure 2) would require
 135 prohibitively large computational resources. To overcome this
 136 constraint, a simplified 3D FEM model was built with one
 137 single principal shaft and a simplified geology. A dynamic
 138 analysis with the seismic load was performed for this simplified
 139 model, which lasted approximately two weeks. Once the
 140 structural and soil responses were computed, an analysis of the
 141 main deformation modes and internal stresses of the structure
 142 was performed. To replicate these results with a static model, a
 143 set of prescribed displacements (applied at the boundaries of the
 144 model) was iteratively calibrated. Finally, this set of prescribed
 145 displacements was applied to the complex full design model to
 146 estimate the seismic response of the entire structure, including
 147 the four shafts and the connecting tunnels.

148 3.2 Complex full design model

149 To create the initial static design, a complex full 3D model was
 150 developed, using a Hardening Soil Model with Small Strain
 151 Stiffness (HSS) for the soil. Each principal shaft consisted of 56
 152 plates that simulated the individual wall sections (thickness:
 153 1.5 m), and six ring beams (thickness: 3 m), distributed at
 154 different heights of the shaft (0 m, -14.5 m, -29.5 m, and -47 m
 155 below ground level), to increase its structural stiffness. This
 156 design considered only ring beams and no other stiffening
 157 element (e.g. struts), as they were not feasible due to technical
 158 requirements. The foundation slab was modelled with a
 159 thickness of 4 m and the foundation piles with a diameter of
 160 1.5 m in a 3 m x 3 m grid below the foundation slab. All wall
 161 and beam structural members of the shaft were modelled as
 162 plate elements, while the foundation piles were modelled as
 163 embedded beam elements. The material type was set as
 164 isotropic elastic C30/37 partially cracked concrete (i.e. stiffness
 165 calculated as 2/3 of the concrete's nominal stiffness:
 166 22E6 kN/m²). The size of the model is shown in Figure 4.

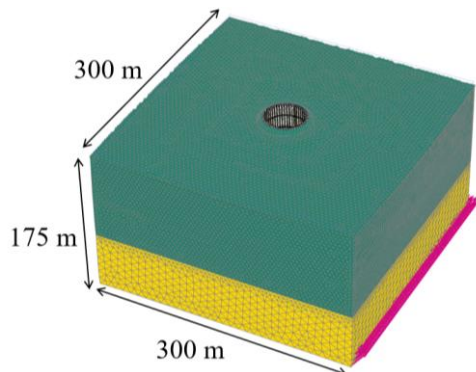


167 Figure 4. Complex full design model.
 168

169 The excavation phases were considered in steps of 5 m of
 170 depth, until reaching the bottom edge of the foundation slab at
 171 -63 m below ground level. The logistic shafts were excavated
 172 first, followed by the main ones. Lastly, the connection tunnels
 173 were constructed. The construction was divided into a total of
 174 39 phases, with one initial phase for gravity loading of the soil.

175 3.3 Simplified model and dynamic analysis

176 As mentioned previously, a simplified version of the model,
 177 following the low-fidelity approach mentioned by Robinson et
 178 al. (2008), was constructed. The geology was simplified into
 179 three main soil layers (soft silt/sand, dense sand, and rock), the
 180 domain depth was reduced (for computational reasons), and one
 181 single principal shaft was considered (Figure 5). The shaft
 182 structure (i.e. the D-wall plates, ring beams, foundation slab,
 183 and pile elements) had the same material properties and
 184 dimensions as in the complex model. The soil parameters for
 185 the HSS constitutive model are shown in Table 2.



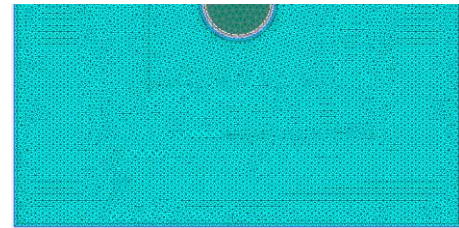
186 Figure 5. Simplified model (green: soft soils; yellow: rock).
 187

188 Table 2. HSS soil parameters for the simplified model.

Soils:	Soft silt/sand	Dense sand	Rock	Units
Depth	0 - 63	63 - 107	> 107	m
γ	20	20	20	kN/m ³
E_{s0}^{ref}	2E3	15E3	300E3	kN/m ²
E_{oed}^{ref}	2E3	15E3	300E3	kN/m ²
E_{ur}^{ref}	5E3	45E3	900E3	kN/m ²
ν_{ur}	0.2	0.2	0.25	-
m	0.9	0.9	0.5	-
p_{ref}	100	100	100	kN/m ²
G_0^{ref}	7.5E3	6.75E4	1.35E6	kN/m ²
$\gamma_{0.7}$	0.1E-3	0.1E-3	0.1E-3	-
c'_{ref}	10	5	50	kN/m ²
ϕ'	25	30	25	°
ψ'	0	0	0	°

189 3.3.1 Discretization

190 To simulate the shear wave propagation in the different soil
 191 layers, the maximum length of an element $h_{e,max}$ was chosen
 192 following the criteria of $h_{e,max} = v_s / 5f_{max}$, with v_s as the shear
 193 velocity and f_{max} as the maximum frequency of the seismic input
 194 motion (Bakr & Ahmad, 2018). The shear wave velocity for the
 195 softest soil layer (180 m/s) and the frequency of 10 Hz for the
 196 seismic input motion were used, obtaining a maximum element
 197 length of 3.6 m. A mesh with 540k elements was generated.



198 Figure 6. Fragment (domain's symmetric half) of the mesh.
 199

200 3.3.2 Dynamic boundary conditions

201 For the seismic analysis, dynamic boundary conditions (BC)
 202 were implemented to simulate the dynamic response of the soil
 203 domain. A free-field BC was chosen for the side boundaries, a
 204 compliant base BC was chosen for the bottom boundary, and no
 205 specific BC was selected for the top boundary. These BC are
 206 the ones applicable for dynamic time history analysis in Plaxis
 207 3D (Bentley, 2024). The seismic surface displacement
 208 multipliers (following the seismic input motion shown in
 209 Figure 2) were applied to the bottom boundary in all three
 210 spatial directions.

211 3.4 Calibration of prescribed displacements

212 Once the results of the dynamic simulation were obtained, an
 213 analysis of the most relevant displacements and internal forces
 214 in the shaft was performed. Using these results, a set of
 215 prescribed displacements applied on the side boundaries was
 216 iteratively calibrated by hand. The calibration was performed to
 217 achieve a similar order of magnitude of (i) deformations, (ii)
 218 internal forces (normal forces and bending moments), and (iii)
 219 to reproduce a similar deformation shape (i.e. shearing,
 220 bending, or a combination of both) compared to the one
 221 computed in the dynamic analysis.

222 3.5 Application to the complex full design model

223 The calibrated set of prescribed displacements was then applied
 224 to the complex model to study the response of the complex

225 structure (the four interconnected shafts) to these imposed
 226 prescribed displacements. Therefore, eight combinations
 227 (Table 3) were applied to consider the random multidirectional
 228 nature of the seismic loading and to take into account the
 229 geometric characteristics: a sloped geology and an asymmetric
 230 structure. With these sets of prescribed displacements, the
 231 determinant internal stresses and displacements of the structure
 232 were evaluated and used for preliminary design.

233 Table 3. Prescribed displacement combinations.

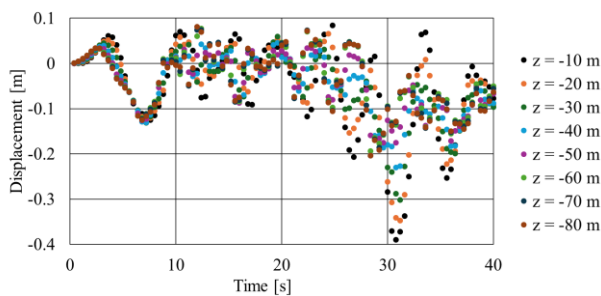
Combination	1	2	3	4	5	6	7	8
x-axis multiplier	-1	+1	0	0	-1	-1	+1	+1
y-axis multiplier	0	0	-1	+1	-1	+1	-1	+1

234 4 RESULTS

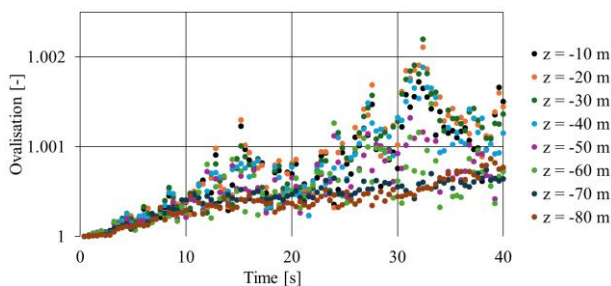
235 4.1 Seismic analysis (DBE)

236 4.1.1 Dynamic analysis (simplified model)

237 This section presents the results of the dynamic analysis run for
 238 the simplified model. The average phase displacements (of all
 239 three spatial directions) of the shaft at different depths below
 240 the ground was analysed (Figure 7). These results show that the
 241 highest average displacements appear at approximately 32 s,
 242 with an order of magnitude of 0.4 m. However, these results do
 243 not indicate whether these displacements correspond to a
 244 shearing, translation, bending, or any other deformation mode.
 245 To estimate the most critical deformations for the shaft
 246 structure, the ovalisation of the shaft during the dynamic
 247 simulation was analysed (Figure 8), which was calculated as the
 248 ratio between the minimum and maximum radii of the deformed
 249 shaft. The ovalisation in the shaft tends to increase with
 250 increasing seismic load, reaching its maximum also at 32 s.
 251 Finally, also the vertical deformation gradient was analysed to
 252 elucidate the most critical vertical bending deformation mode
 253 of the structure.



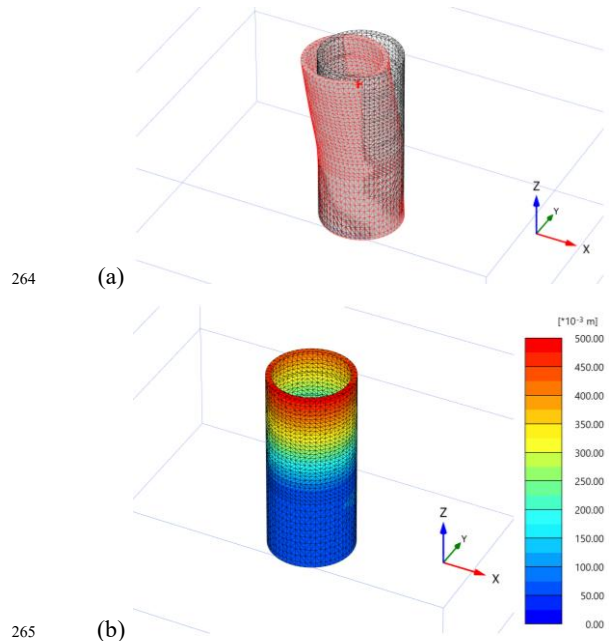
254 Figure 7. Shaft average displacements at different depths z below
 255 ground level.
 256



257 Figure 8. Shaft ovalisation at different depths z below ground level.
 258

259 The deformation shape and magnitude at the relevant time
 260 step of $t = 32$ s (Figure 9) suggests that the structure's bottom is
 261 fixed into the rock, while the top of the structure bends with a

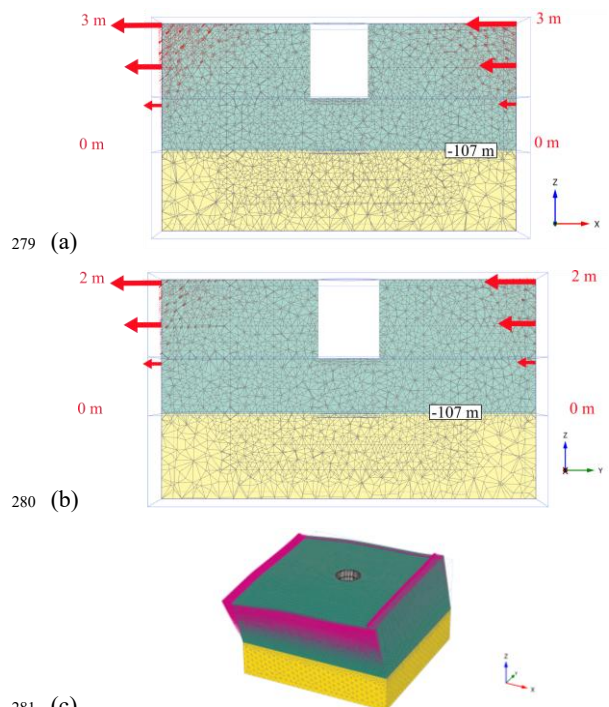
262 peak displacement of 0.5 m. This mode of deformation is thus
 263 bending, and it is comparable to a fixed beam loaded at its end.



265 (b)
 266 Figure 9. Dynamic results ($t = 32$ s): (a) shape and (b) displacements

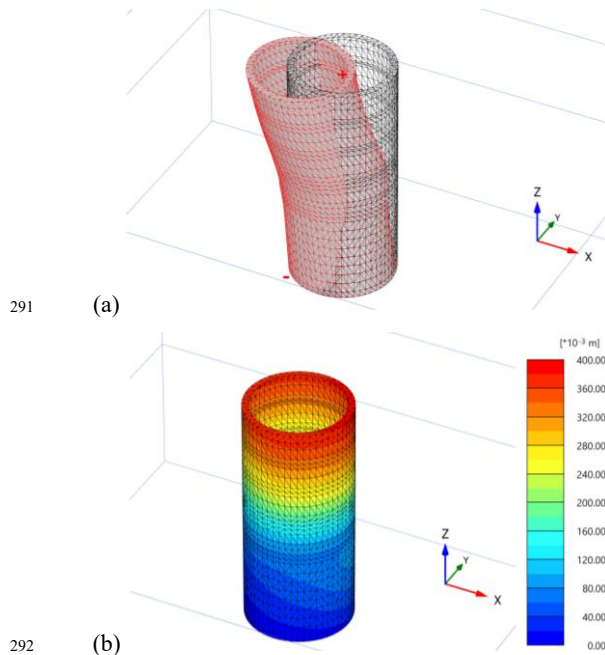
267 4.1.2 Result of the calibration of prescribed displacements

268 As previously indicated, the most critical displacement and
 269 shaft ovalisation takes place at 32 s. The calibration was carried
 270 out for these deformations and internal stresses of the shaft. The
 271 calibrated set of prescribed displacements was applied at the
 272 side boundaries of the model. The rock will not be subject to
 273 substantial deformations (Figure 9), while the softer upper soil
 274 layers will be exposed to increasing shearing with decreasing
 275 confining pressure. Figure 10 shows the iteratively calibrated
 276 prescribed displacements in both directions. It is worth noting
 277 that the displacements were left at 0 m at the boundary zone
 278 between the rock and dense sand layers to prevent soil failure.



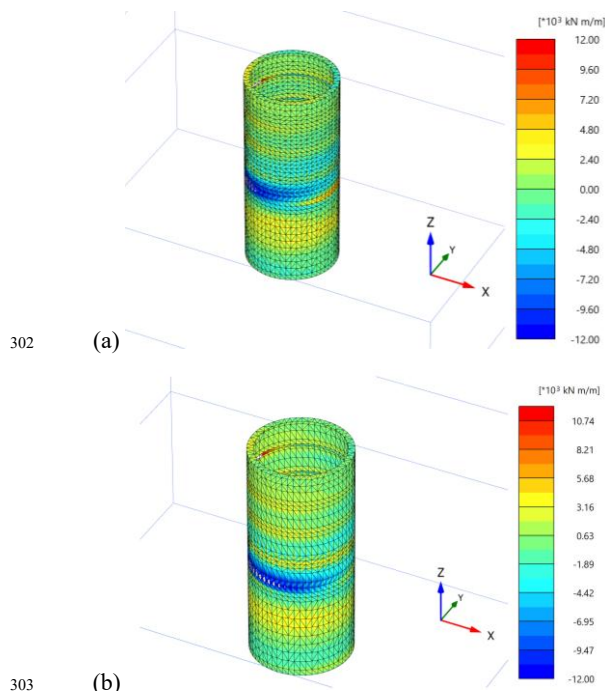
281 (c)
 282 Figure 10. Calibrated prescribed displacements applied to the side
 283 boundaries in (a) x and (b) y directions, and (c) deformed model.

284 Figure 11 shows the results of the shaft structure subject to
 285 the prescribed displacements. These pseudo-static results
 286 (Figure 11) are similar to those obtained via dynamic modelling
 287 (Figure 9) in terms of deformation shape and displacement
 288 magnitudes, with an error in the displacements of the pseudo-
 289 static simulation of roughly 6 %, which was accepted for a
 290 preliminary design stage.



292 (b)
 293 Figure 11. Pseudo-static results (prescribed displacements): (a) shape
 294 and (b) displacements

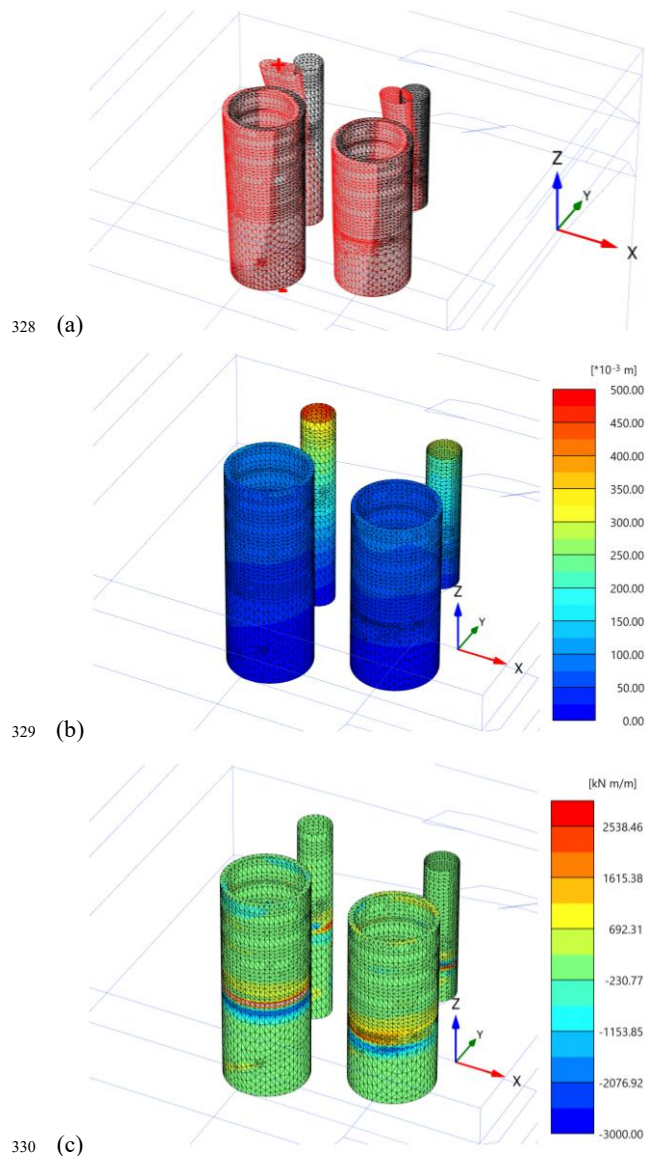
295 The internal forces of the shaft were analysed to compare
 296 the results from the dynamic model and the pseudo-static
 297 simulation. Figure 12 shows the shaft moments (M22) for both
 298 cases. The results are comparable in terms of moment distri-
 299 bution and magnitudes, with an error of 1 to 5 %. Thus, the
 300 calibration was accepted and the prescribed displacements were
 301 applied to the complex model as described in the next section.



303 (b)
 304 Figure 12. Bending moment in the major axis 22 for the (a) dynamic
 305 analysis and (b) pseudo-static (prescribed displacements) simulation

306 4.1.3 Pseudo-static analysis (complex model)

307 The calibrated prescribed displacements were applied to the
 308 complex model in multiple directions (Table 3). Figure 13
 309 shows the deformation shape, magnitude, and the moments
 310 (M22) for the worst-case combination of prescribed
 311 displacements (i.e. #7 according to Table 3). These results
 312 indicate that the seismic action has a significant effect on the
 313 upper part of the structure, with bending and shearing as the
 314 principal deformation modes. In terms of the deformation
 315 magnitude, the maximum displacement is in the order of
 316 0.47 m, principally affecting the logistic shaft with fewer rock
 317 embedment. It is noted that the principal shafts are subjected to
 318 maximum deformations of approximately 0.2 m, which are
 319 considerably less if compared to the dynamic analysis (in the
 320 order of 0.5 m). This is due to the different rock embedment
 321 conditions. The dynamic analysis was performed for the shaft
 322 with the deepest rock level, to account for the most critical
 323 condition. In general, it is observed that the complex structure
 324 reacts stiffer (i.e. with fewer deformations) to the seismic load,
 325 suggesting a potential stiffening effect of the four
 326 interconnected shafts. Moreover, the sloped rock also
 327 contributes to a stiffer response.



330 (c)
 331 Figure 13. Results of the pseudo-static analysis of the complex model
 332 (combination #7): deformation (a) shape and (b) magnitude, and (c)
 333 moments (M22).

334 Regarding the bending moments (M₂₂), it is seen that
 335 moment peaks appear in the regions where stresses are
 336 transferred between structures: e.g. between the shaft and the
 337 foundation slab, between the shaft and the bed rock, and
 338 between the shafts and the tunnels.

339 4.2 Advantages, limitations, lessons learnt and future work

340 The main advantage is that this approach is useful for the
 341 analysis of complex structures under seismic loading, which
 342 would otherwise be very time-consuming to compute. It is
 343 noted that this approach is applicable as a preliminary design
 344 strategy to estimate the order of magnitude of deformations,
 345 stresses or internal forces. However, for very complex
 346 structures or irregular soil layering, the calibrated prescribed
 347 displacements on the simplified model (with plain soil layers)
 348 are not fully applicable to the more complex model (with sloped
 349 soil layers). This is noted as an important limitation, because it
 350 may induce some errors when transferring the prescribed
 351 displacements from the simplified to the complex model.
 352 Moreover, the calibration of prescribed displacements is
 353 conducted manually, based on maximum displacements or the
 354 ovalisation of the structure. It is intended to capture the worst-
 355 case condition; however, due to the nature of manual
 356 calibration, this may also induce slight errors.

357 During the analysis, it has been observed that the domain
 358 dimensions of both models (i.e. complex and simplified) need
 359 to be chosen as equal to simulate the pseudo-static prescribed
 360 displacement application, without inducing errors derived from
 361 the soil's nonlinearity. It was noted that for large, prescribed
 362 displacements applied on the model boundaries, the stresses
 363 were not fully transferred to the structure due to soil failure.
 364 Caution is thus asked when defining the parameters subject to
 365 simplification during surrogate modelling. Furthermore, it is
 366 recommended to verify potential simplifications through
 367 sensitivity analyses.

368 As mentioned previously, the calibration of the prescribed
 369 displacements is time-consuming since it is carried out
 370 manually, which might be also linked with slight errors. To
 371 improve this approach, an automatised calibration will be
 372 implemented in future phases, following previous research on
 373 automatised calibration via optimisation algorithms as
 374 presented in Meier & Pitteloud (2024).

375 5 CONCLUSIONS

376 This paper presents the application of an existing methodology,
 377 originally developed for tunnels, to different underground
 378 structures (i.e. multiple interconnected deep shafts). This
 379 methodology consists of calibrating a set of prescribed
 380 displacements from a dynamic analysis based on a simplified
 381 model. These prescribed displacements are later applied to a
 382 pseudo-static analysis of a complex full design model. With this
 383 approach, the seismic analysis of complex underground
 384 structures and soils (i.e. soft saturated soils) become feasible
 385 and achievable in terms of computational power. Based on the
 386 example of a case study, this approach has shown that it is
 387 effective in estimating displacements and stresses of the
 388 underground structures under seismic events. Even though it
 389 presents some limitations, this approach is recommended for a
 390 preliminary design strategy. Moreover, it should be used as an
 391 example of how complex problems in new fields may be solved
 392 by applying existing techniques, while keeping the
 393 computational demand under reasonable limits.

394 6 ACKNOWLEDGEMENTS

395 We would like to gratefully acknowledge Prof. Ioannis
 396 Anastasopoulos (ETH Zurich), Thomas-Michael Baltzer,

397 Dr. Andrea Abati, Dr. Ivan Stojnić, Paul Robinson, Martin
 398 Stache, Dr. Martin Bieri, and co-workers from the Gruner and
 399 Gruner Stucky Groups, for their expertise and advise on this
 400 project.

401 7 REFERENCES

- 402 Asher, M.J., Croke, B.F.W., Jakeman, A.J., Peeters, J.M. 2015. A
 403 review of surrogate models and their application to groundwater
 404 modeling. *Water Resources Research*, 51, 5957-5973.
 405 Bakr, J., Ahmad, S.M. 2018. A finite element performance-based
 406 approach to correlate movement of a rigid retaining wall with
 407 seismic earth pressure. *Soil Dynamics and Earthquake*
 408 *Engineering*, 114, 460-479.
 409 Bentley. 2024. *Tutorial Manual Plaxis 3D 2024.2*. 07/2024.
 410 Gaspari, G.M., Quaglio, G., Floria, V. 2011. Design and construction
 411 of tunnels under severe seismic conditions. The case of Kadikoy-
 412 Kartal metro line in Istanbul. *Rivista Italiana di Geotecnica*
 413 *2/2011*.
 414 Hashash, Y.M.A., Hook, J.J., Schmidt, B., Yao, J.I.C. 2001. Seismic
 415 design and analysis of underground structures. *Tunneling and*
 416 *Underground Space Technology*, vol. 16, 247-293.
 417 Liu, Z., Fang, Q., Shen, Y., Ai, Q., Wang, H., Huang, X., Yuan, Y.
 418 2024. Two-stage surrogate modeling strategy for predicting
 419 foundation pit excavation-induced strata and tunnel deformation.
 420 *Tunneling and Underground Space Technology*, vol. 151, 105845.
 421 Meier, J., Rudolph, S., Schanz, T. 2009. Effective algorithm for
 422 parameter back calculation – Geotechnical Applications.
 423 *Bautechnik*, vol. 86 (S1), pp. 86-97.
 424 Meier, J., Pitteloud, L. 2024. Optimierung von geotechnischen
 425 Bauwerken auf der Grundlage von numerischen Modellen.
 426 In: Geotechnik Schweiz, *Proc. Frühjahrstagung Numerik /*
 427 *Modélisation numérique*. Yverdon-les-Bains, 2024.
 428 Pescara, M., Gaspari, G.M., Repetto, L. 2011. Design of underground
 429 structures under seismic conditions: a long deep tunnel and a
 430 metro tunnel. *ETH Zurich Colloquium on seismic design of*
 431 *tunnels*.
 432 Robinson, T., Eldred, M.S., Willcox, K.E., Haines, R. 2008. Surrogate-
 433 based optimization using multifidelity models with variable
 434 parameterization and corrected space mapping. *American Institute*
 435 *of Aeronautics and Astronautics Journal*, 46(11), 2814-2822.
 436 St John, C.M., Zahrah, T.F. 1987. A seismic design of underground
 437 structures. *Tunneling and Underground Space Technology*, vol. 2,
 438 No. 2, pp. 165-197.
 439 Wang, J-N., Munfakh, G.A. 2001. Seismic design of tunnels.
 440 *Transactions on the Built Environment*, vol 57, ISSN 1743-3509.
 441 Zheng, H., Mooney, M., Gutierrez, M. 2023. Surrogate model for 3D
 442 ground and structural deformations in tunneling by the sequential
 443 excavation method. *Computers and Geotechnics*, vol. 154,
 444 105142.